Los Alamos National Laboratory is operated by the University of California for the United States Department of Energy under contract W-7405-ENG-36.

Wave interaction solutions

Los Alamos
Los Alamos National Laboratory
Los Alamos, New Mexico 87545

Edited by Sharon L. Crane
Photocomposition by Mary Louise Garcia

LA-9119

UC-45
Issued: January 1982

Plane Wave Generator Calculations

George H. Pimbley
Charles L. Mader
Allen L. Bowman

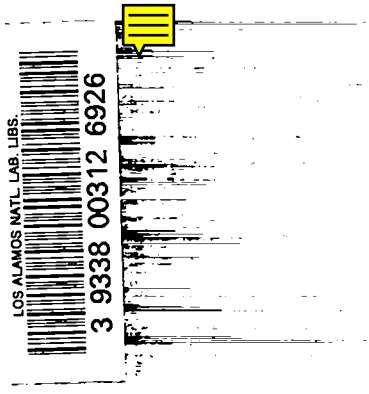

Los Alamos National Laboratory
Los Alamos, New Mexico 87545

PLANE WAVE GENERATOR CALCULATIONS

by

George H. Pimbley, Charles L. Mader, and Allen L. Bowman

ABSTRACT

Three plane wave generators (the P-040, P-081, and P-120) have been studied experimentally and theoretically. Significant pressure gradients across the lenses and behind the wave surfaces are present even though the surface of the detonation wave is planar.

I. INTRODUCTION

Three types of plane wave generators make use of the properties of Baratol and Comp B to form effective lenses. Baratol's slow detonation velocity and Comp B's high detonation velocity, if used in the proper configuration, can convert a spherically diverging wave into an approximate plane wave. The P-040, P-081, and P-120 plane wave generators are now in use at Los Alamos National Laboratory.

Of these, the P-040 has the simplest design, consisting of an inverted right circular Baratol cone encased in a coaxial Comp B cylinder (see Fig. 1). The Baratol cone has a slightly rounded apex. Thus the top face of the assembly consists of Baratol; the bottom surface is Comp B. This device is detonated axially symmetrically from beneath. The detonator is customarily much smaller in diameter than the upper assembly and is often encased in Comp B, making a uniform cylinder; we assumed this in our calculations.

The P-081 and P-120 generators each retain the inner Baratol cone, but they are larger and heavier than the P-040. These two generators each consist of two coaxial cones of explosive (see Fig. 2). The inner Baratol cone is encased in an outer conical Comp B shell. The outer conical shell is truncated, but it covers the rounded apex

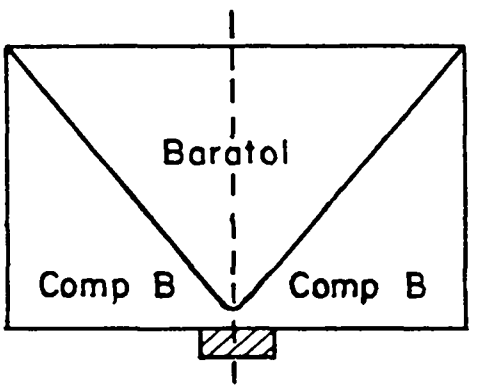

Fig. 1. P-040 generator.

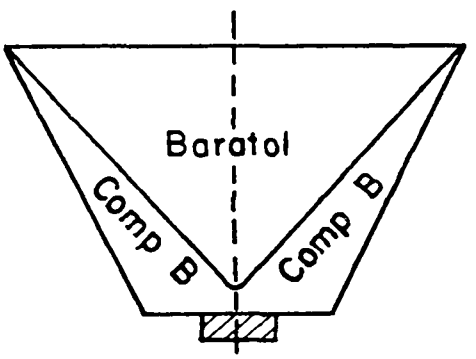

Fig. 2. P-081 or P-120 generator.

of the Baratol with a separation distance. The detonator is smaller in diameter than the truncated end of the upper assembly, and it is often encased in Comp B.

Each plane wave generator is designed to produce a plane shock wave at the upper Baratol surface of the device. The generators use the lens effect of a Baratol cone, and the lower transit velocity therein, to mold the somewhat spherical spreading detonation waves into planar patterns as they rise.

II. SIMULATION DESCRIPTIONS

The 2DE reactive Eulerian hydrodynamics code was used in these calculations.[1] Reference 2, pp. 29-32, details how this code was used in another situation.

A. Simulation of the P-040 Generator

The calculation plan is shown in Fig. 3. The problem domain, a vertical half-slice through the cylinder axis, is divided into 12 rectangular regions, with materials as shown. In the initial setup of the calculation, Comp B is the prescribed material throughout regions 4, 5, 7, and 8. The Baratol in regions 7 and 8 is laid over the Comp B above the diagonal, using special modification of the circular input provision in the 2DE code (Ref. 1, p. 36, and Ref. 2, p. 31). This modification requires an additional subroutine (called CONE 1) in the NITCELL section of 2DE. Burned Comp B with C-J energy and density is also substituted in region 4 to form the hot-spot detonator. The dimensions given in Fig. 3 (in centimeters) are those used in the calculation.

On the left in Fig. 3, an axial boundary condition is given. The continuation boundary condition is prescribed on the other three boundaries of the rectangular domain (Ref. 2, pp. 29-30).

The Comp B and Baratol explosives were burned using the C-J volume burn technique.

B. Simulation of the P-081 Generator

In Fig. 4 we present the P-081 calculation plan. The domain is again a vertical half-slice through the z-axis (cylindrical symmetry) and is divided into 20 rectangular regions, with materials as shown. Initially, air is the

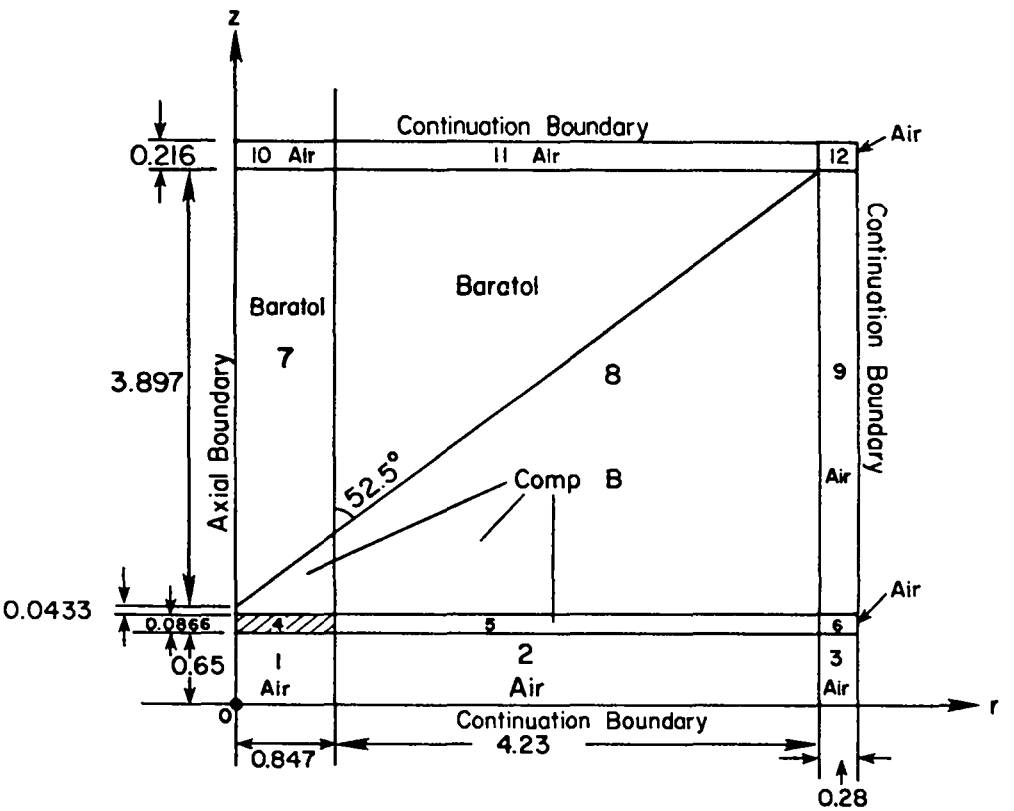

Fig. 3. Plan of the P-040 calculation (dimensions given in centimeters).

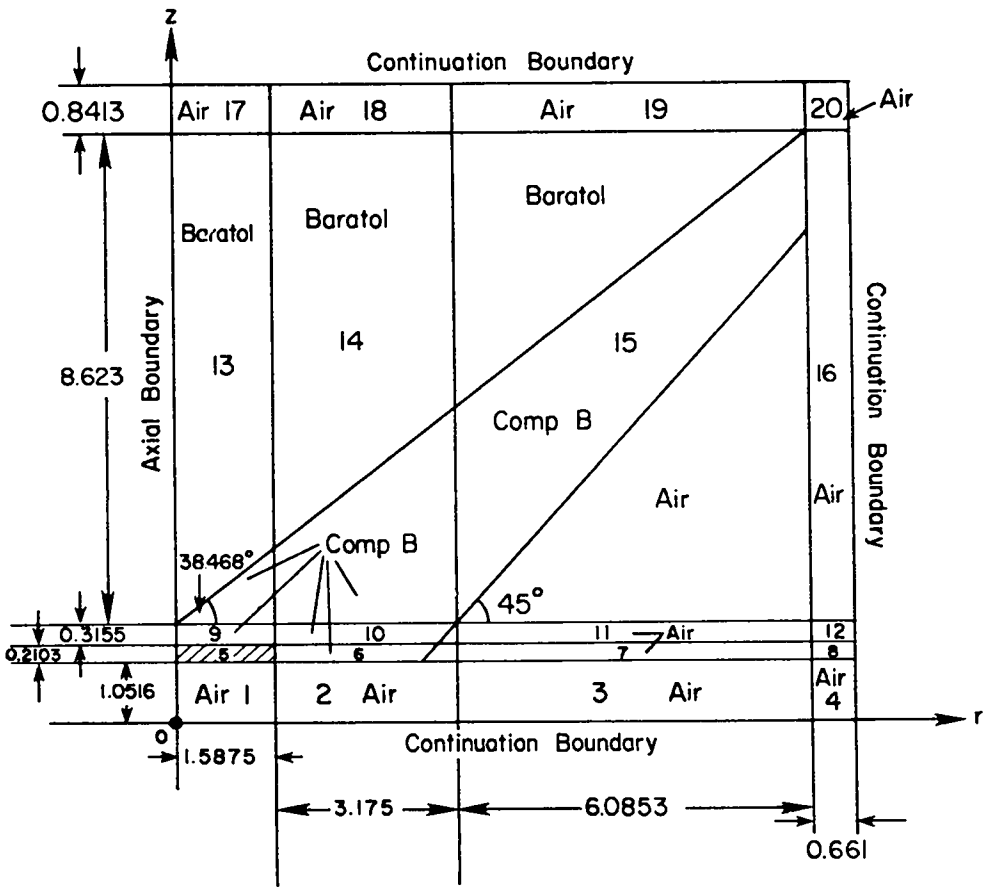

Fig. 4. Plan of the P-081 calculation (dimensions given in centimeters).

prescribed material throughout all regions in Fig. 4. Then, by using CONE 2, an added subroutine in the NITCELL section of the 2DE code, the Comp B is laid over the air above the 45° diagonal in regions 5, 6, 9, 10, and 13 through 15. Again (using CONE 2), Baratol is laid over the Comp B in regions 13 through 15 above the 38.468° diagonal. Burned Comp B, with C-J density and energy, is substituted for the solid Comp B in region 5 to form the hotspot detonator. The dimensions given in Fig. 4 (in centimeters) are those in the final calculation.

An axis boundary condition is posed on the left in Fig. 4 (see Ref. 2, pp. 29-30); continuation boundary conditions are prescribed on the other three boundaries of the problem rectangle. Again, the C-J volume burn technique is used.

C. Simulation of the P-120 Generator

The setup for the P-120 computer simulation is like that used for the P-081 generator. Apart from dimensions and angles, the simulation differed in the addition of an aluminum plate to the top of the assembly so as to match the actual experiment.[4] The CONE 2 subroutine is used in the same way.

Figure 5 shows the P-120 calculation plan, where the added aluminum plate is accommodated by dividing the problem rectangle into 24 regions. Initially, regions 1 through 16 are air-filled, regions 17 through 19 contain aluminum, and regions 20 through 24 are also air-filled. Next, Comp B is laid over the air in regions 5, 6, 9, 10, and 13 through 15, above the 42° line, using the added CONE 2 routine. Baratol is laid over the Comp B in regions 13 through 15 above the 40° diagonal. Burned Comp B, with C-J energy and density, is substituted in region 5 to form the hot-spot detonator, again with the CONE 2 subroutine.

In Fig. 5 the axis boundary condition is imposed on the left boundary, whereas the continuation boundary condition is prescribed on the three remaining rectilinear boundaries. The C-J volume burn technique is used to burn the Comp B and the Baratol. The dimensions (in

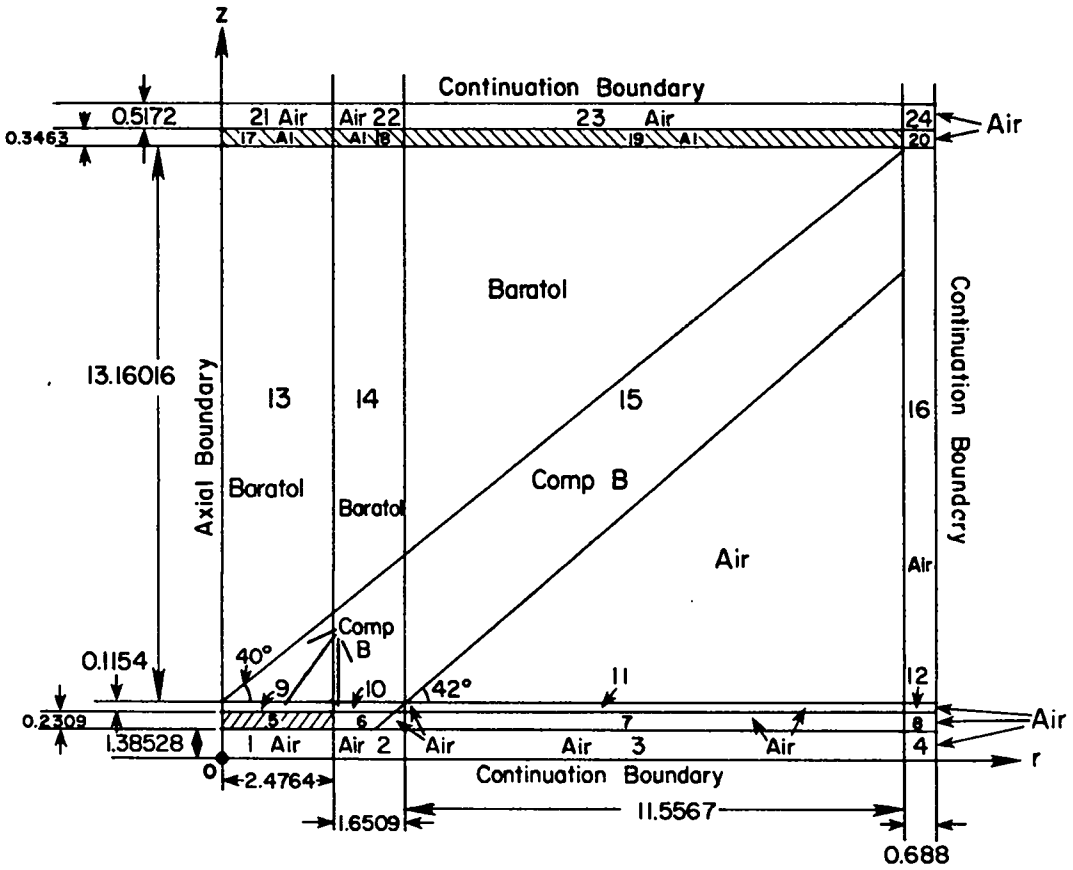

Fig. 5. Plan of the P-120 calculation (dimensions given in centimeters).

centimeters), given in Fig. 5, and the angles are those used in the final calculation.

III. COEFFICIENTS AND OTHER DATA TABLES

The coefficients and methods used to compute the curve fits for the HOM equations of state are discussed in the 2DE manual (Ref. 1, pp. 22-28). Nomenclature is given in the same source (pp. 32-38). Useful discussion is also found in Ref. 2, pp. 27-52. The conventions used in these sources will be followed here, excepting our use of the circle routines in the 2DE code to compute cones.

The following were common to all three of the calculations.

A. Equation-of-State Constants

1. Equation of State for Air.

S (13,1) = 865.224, S(17,1) = 300, S(18,1) = 1×10^{-6}

G (1,1) = −4.50602542688, −1.546110628, −0.003746600292, 0.012392923674

G (5,1) = −0.00207694122929, −1.62655447438, 0.0905283146618, 0.00269004997726

G (9,1) = $-5.43583122192 \times 10^{-5}$, $-1.58521895338 \times 10^{-6}$, 8.22644581441, −0.25152513095

G (13,1) = −0.0134446940047, 0.0140871016422, −0.00218132189985, 0.5, 0.1

2. Equation of State for Comp B

S (1,2) = 0.231, 1.83, 0.01, 0., 0., −8.86750780814, −79.7357471516

S (8,2) = −159.438975952, −135.411036759, −39.127465595, 1.5, 0.259

S (13,2) = 0.583090379009, 5×10^{-5}, 0., 0., 300., 1×10^{-6}

G (1,2) = −3.52584878974, −2.33429189056, 0.597267325606, $3.04510424546 \times 10^{-3}$

G (5,2) = −0.1752264031, −1.56087684485, 0.533121475935, 0.0806310874142

G (9,2) = 3.33816891056 × 10^{-3}, −6.84399991171 × 10^{-4}, 7.5027805855, −0.441209000835
G (13,2) = 0.151292636188, 0.0677883292739, −0.0242403364371, 0.5, 0.1
G (18,2) = 0.745, −3.88984471, −1.471507496, 0.47986951, 7.456816382
G (23,2) = −0.259821396, G(26,2) = −5.116, G(27,2) = −0.05466937122

3. Equation of State for Baratol.

S (13,3) = 0.384, S(17,3) = 300, S(18,3) = 1 × 10^{-6}
G (1,3) = −6.76099488335, −3.96, 0., 0., 0.
G (6,3) = −1.87989615929, 2.90771932643 × 10^{-1}, 6.60456508993 × 10^{-2}
G (9,3) = 6.83006286414 × 10^{-3}, 2.65738014600 × 10^{-4}
G (11,3) = 0.0, −1.968, 0.0, 0.0, 0.0, 0.5, 0.1

4. Equation of State for Aluminum (used for P-120 only).

S (1,4) = 0.535, 1.35, 0.01, 0., 0., −20.7547507908, −115.617830366
S (8,4) = −177.762573069, −114.252754176, −25.6423794962, 1.7, 0.22
S (13,4) = 0.35906642729, 2.4 × 10^{-5}, 10.0, 0.1, 300.0, 1.0 × 10^{-6}

B. Other Quantities

1. Artificial Viscosity Constants.

Air: 0.2, Comp B: 0.15, Baratol: 0.1

2. Initial Values of Dependent Variables.

Air: RHO = 0.00115577 g/cm^3
I0 = 0.0024668, P0 = 1 × 10^{-6}, T0 = 300 K, U0 = 0., V0 = 0., W0 = 0
Comp B: RHO = 1.713 g/cm^3
I0 = 0.0, P0 = 1 × 10^{-6}, T0 = 300 K, U0 = 0.0, V0 = 0,0, W0 = 1.0, VCJ = 0.4198
Baratol: RHO = 2.604 g/cm^3
I0 = 0.0, P0 = 1 × 10^{-6}, T0 = 300 K, W0 = 1.0, VCJ = 0.3066
Hot-Spot Comp B: RHO = 2.358491 g/cm^3
I0 = 0.02436191, P0 = 1 × 10^{-6}, T0 = 300 K, U0 = 0.0, V0 = 0.0, W0 = 0.0
Aluminum: RHO = 2.785 g/cm^3
I0 = 0.0, P0 = 1 × 10^{-6}, T0 = 300 K, W0 = 1.0

3. Increments. The time and space increments differ with each generator.

P-040 Calculations: DELR = 0.0564444 cm, DELZ = 0.043313 cm, DELT = 0.0105 μs
P-081 Calculations: DELR = 0.13229 cm, DELZ = 0.10516 cm, DELT = 0.02103 μs
P-120 Calculations: DELR = 0.13758 cm, DELZ = 0.1154433 cm, DELT = 0.02639225 μs

IV. NUMERICAL SIMULATION RESULTS

A. Results for the P-040 Generator

1. Comparison with Radiographic Information. Experimental information available for comparison with computed results is given in Ref. 3, pp. 380-387 and 402-409. This reference shows two sets of radiographs with four shots in each set. Each of these series of four x-ray shots depicts sequentially the events in an actual P-040 plane wave generator during a test. The shock wave progress is shown at four discrete times as it rises in the cone after the initial detonation. When interpreting these radiographs, note that we are observing a two-dimensional projection of a three-dimensional event, with consequent information loss.

The data sheet accompanying each set of radiographs[3] gives dimensions that are useful for matching the PHERMEX experiments with our calculations. The radiographic times and beam axis heights given are relevant mainly for experimenters. These radiographic times were used, however, for inferring the time increments between successive shots and in selecting our computational time increment, DELT = 0.0105 μs. Thus we matched our computational sequencing with the experimental sequencing, although the respective initial times differed.

Figures 6a-d show density contour plots at 2.625, 4.725, 6.825, and 7.665 μs, respectively. The radius is plotted horizontally and axial z is plotted vertically. The Baratol cone remains approximately static throughout the sequence, but it is permeated progressively by wave activity, as shown by the growing array of density contours. Steepness of density gradients can be assessed by closeness of contours.

The circles on Figs. 6a-c mark the experimental points read from the actual radiographs and correlated in time with the numerical calculation.

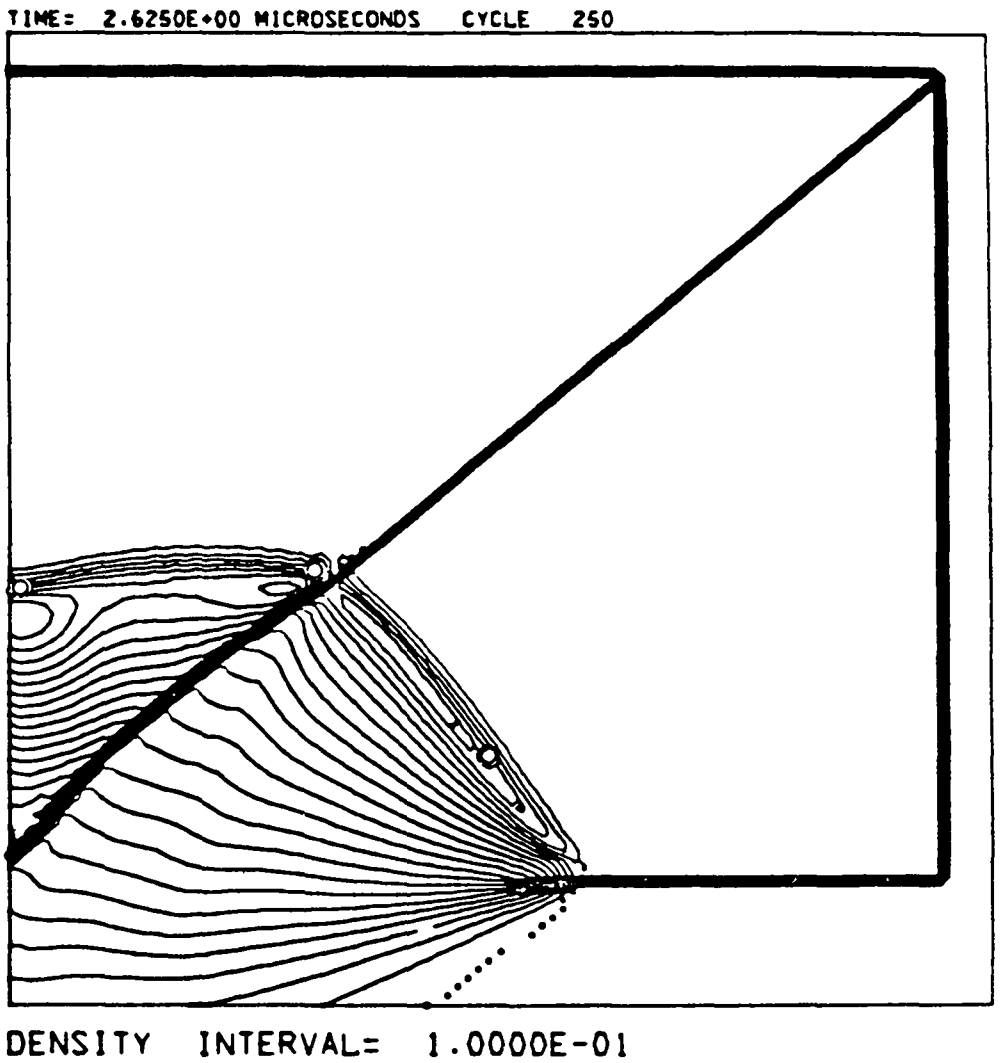

Fig. 6a. Density contour plots at 2.625 μs (P-040).

2. **Plane Wave Arrival at the Top.** We have described the radiographs as two sets, each having four x-ray pictures representing the shock wave density behavior at four sequential times. The first three of these times correspond with the first three plots of Fig. 6, derived from actual 2DE computation. The fourth radiograph of each set is useless for inference because the wave has reached the free surface of the lens. The corresponding computational time is approximately 7.665 μs. We rely on the computed results as shown in Figs. 7 and 8 for conditions at the top of the P-040 generator.

Figure 7 shows four simultaneous, one-dimensional plots of pressure versus z (the axial coordinate), obtained for R = 0.02822, 1.2136, 2.5118, and 3.6407 cm, respectively, at t = 7.665 μs. It cross-sections across the top of the P-040 emerging pressure wave shape found by our calculations. Figure 8 is a two-dimensional pressure contour plot at t = 7.665 μs. The pressure gradient for the arriving wave varies across the lens, and we see a degree of planarity characteristic of the P-040 design.

3. **Conclusions for the P-040 Generator.** The computer simulation agrees with the experimental PHERMEX data with respect to arrival times of the detonation wave. The waves emerge almost planar, but with a significant pressure gradient across the lens according to the calculations.

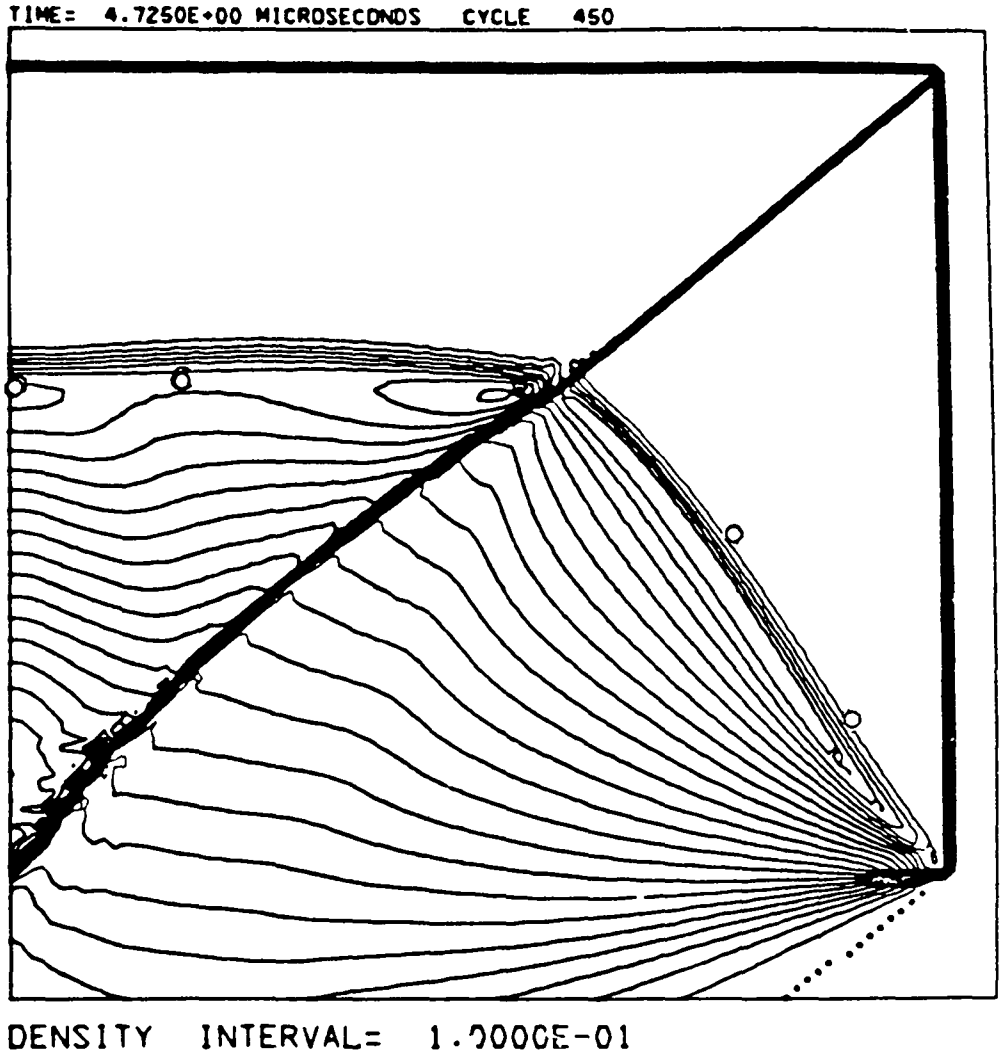

Fig. 6b. Density contour plots at 4.725 μs (P-040).

B. Results for the P-081 Generator

The small amount of radiographic information available now,[3] on the processes within the P-081 generator during an actual shot, is unsuitable for comparison with our 2DE calculations on this device. Consequently, we present only selected density contour plots during the computer simulation, and we discuss, as well as possible, the detonation wave as it reaches the top of the assembly.

1. Selected Plots and Contours. In Figs. 9a-e, we present density contour plots at 2.103, 5.2575, 9.4635, 13.669, and 17.35 μs, respectively, again with the radius plotted horizontally and the axial z-coordinate plotted vertically. The Baratol cone, delineated by the upper 38.468° diagonal, remains approximately the same throughout the simulation. The cone is penetrated progressively by wave activity, however, as shown by the growing array of density contours as we proceed from Fig. 9a. The density gradients relate directly to the closeness of the contours.

2. Plane Wave Arrival at the Top. Again, we have no radiographic information on performance of the P-081 generator, so we cannot sequence the times in Fig. 9 with corresponding experiments. The computations show, however, that the approximate flat wave reaches the top

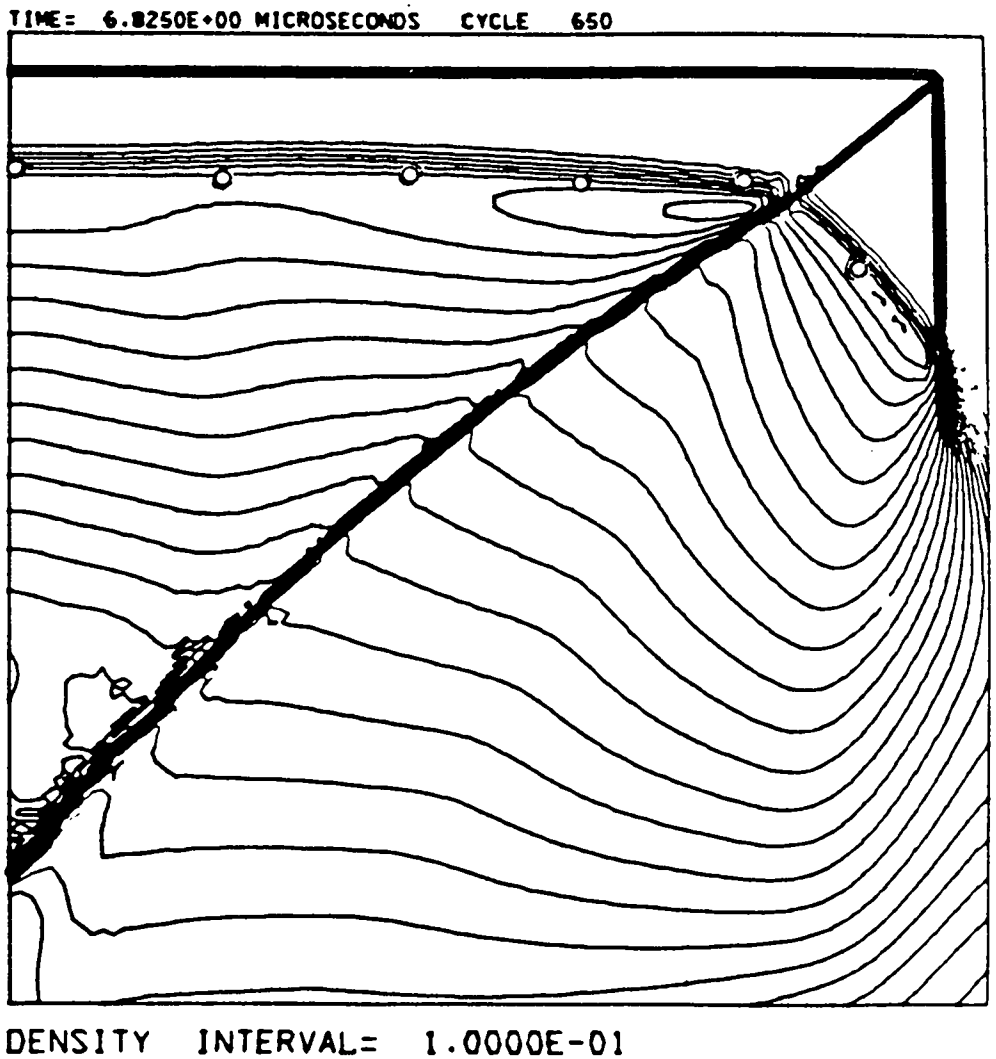

Fig. 6c. Density contour plots at 6.825 μs (P-040).

at about 17.35 μs. The computed results shown in Figs. 10-12 indicate how the detonation wave behaves as it reaches the top of the device.

Figure 10 shows four simultaneous, one-dimensional plots of pressure versus z (that is, pressure along the axis of symmetry) obtained for the radii R = 0.066145, 2.8442, 5.8869, and 8.5327 cm, respectively, at t = 17.35 μs. Figure 11 shows simultaneous vertical flow velocities for the same radial locations at t = 17.35 μs. This sectional overview of the arriving wave shapes is across the top of the P-081 and shows both pressure and velocity. Figure 12 is a two-dimensional plot of the P-081 pressure contours at t = 17.35 μs. Significant differences in the pressure gradient across the lens are calculated, as shown in Fig. 10. The shock wave is highly planar at the top.

3. Conclusions for the P-081 Generator. Although we have no PHERMEX radiographic data that can be compared readily with the density contours in Fig. 9, the waves emerge planar at the top. There is a significant pressure gradient across the lens.

C. Results for the P-120 Generator

As yet, we have no radiographic information on the internal processes during a shot with the P-120 plane

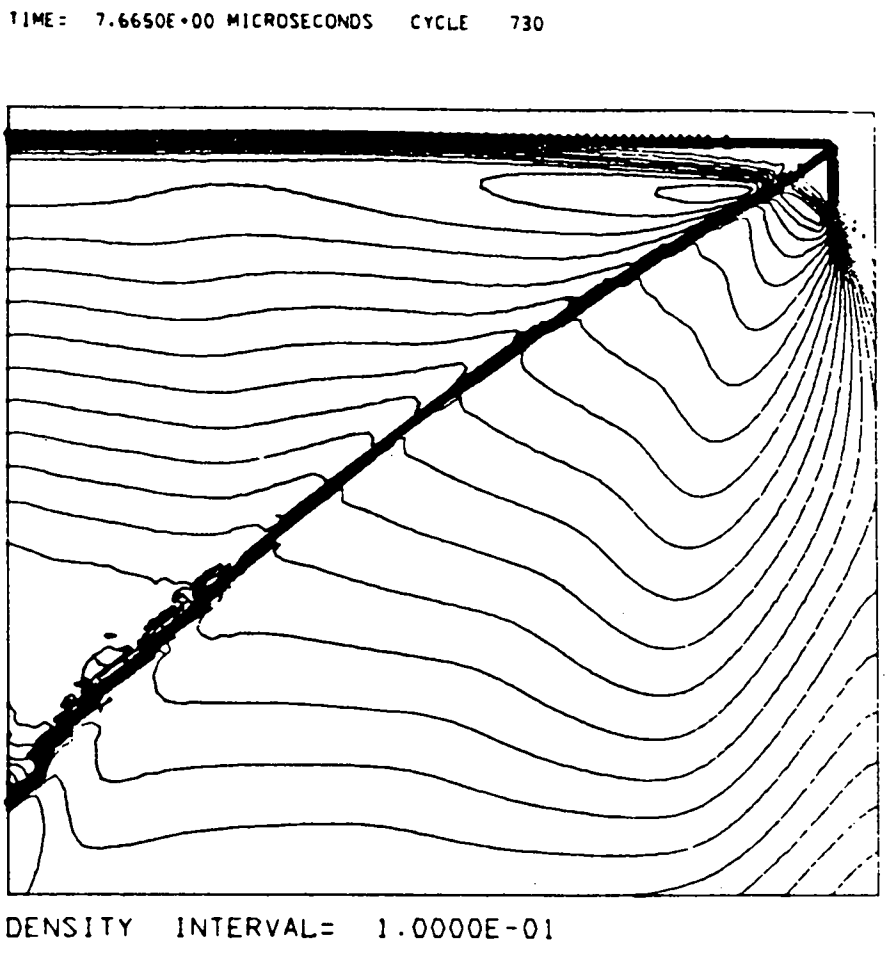

Fig. 6d. Density contour plots at 7.665 μs (P-040).

wave generator. Ramsay[4] has examined the free-surface velocity of a thin aluminum plate that is driven by a P-120 lens and his findings will be mentioned later.

1. **Selected Plots and Contours.** First, we present selected density contours during the computer simulation of the P-120 generator. Then we discuss what happens when the progressively flat wave hits the aluminum plate at the top of the device.

In Fig. 13 we give density contours at 1.3196, 6.5981, 11.877, 17.155, 21.114, and 25.732 μs, with axial z-coordinate plotted vertically and radial coordinate horizontally. Note the aluminum plate at the top of these plots, just under the heavy horizontal line showing where the upper air cushion begins. In the succeeding plots, Figs. 13a-f, the Baratol cone, the Comp B shell, and the air below the 42° line are being affected more and more by the advancing wave activity. Again, the density gradients relate directly to the closeness of the contours.

2. **Plane Wave Arrival at the Aluminum Plate.** The approximate plane wave front reaches the plate at about 25.732 μs. The plots shown in Figs. 14 through 16 describe the arrival of the detonation wave.

Figure 14 shows four simultaneous, one-dimensional plots of pressure versus z in the direction of the z-axis. These were obtained at radii R = 0.06879, 2.958, 6.1223, and 8.8739 cm, respectively, at t = 25.732 μs. Figure 15 shows simultaneous vertical flow velocity for the same set of radii, again at t = 25.732 μs. Figure 16 is a two-dimensional plot of the pressure contours in the P-120 generator at t = 25.732 μs. The pressure wave in

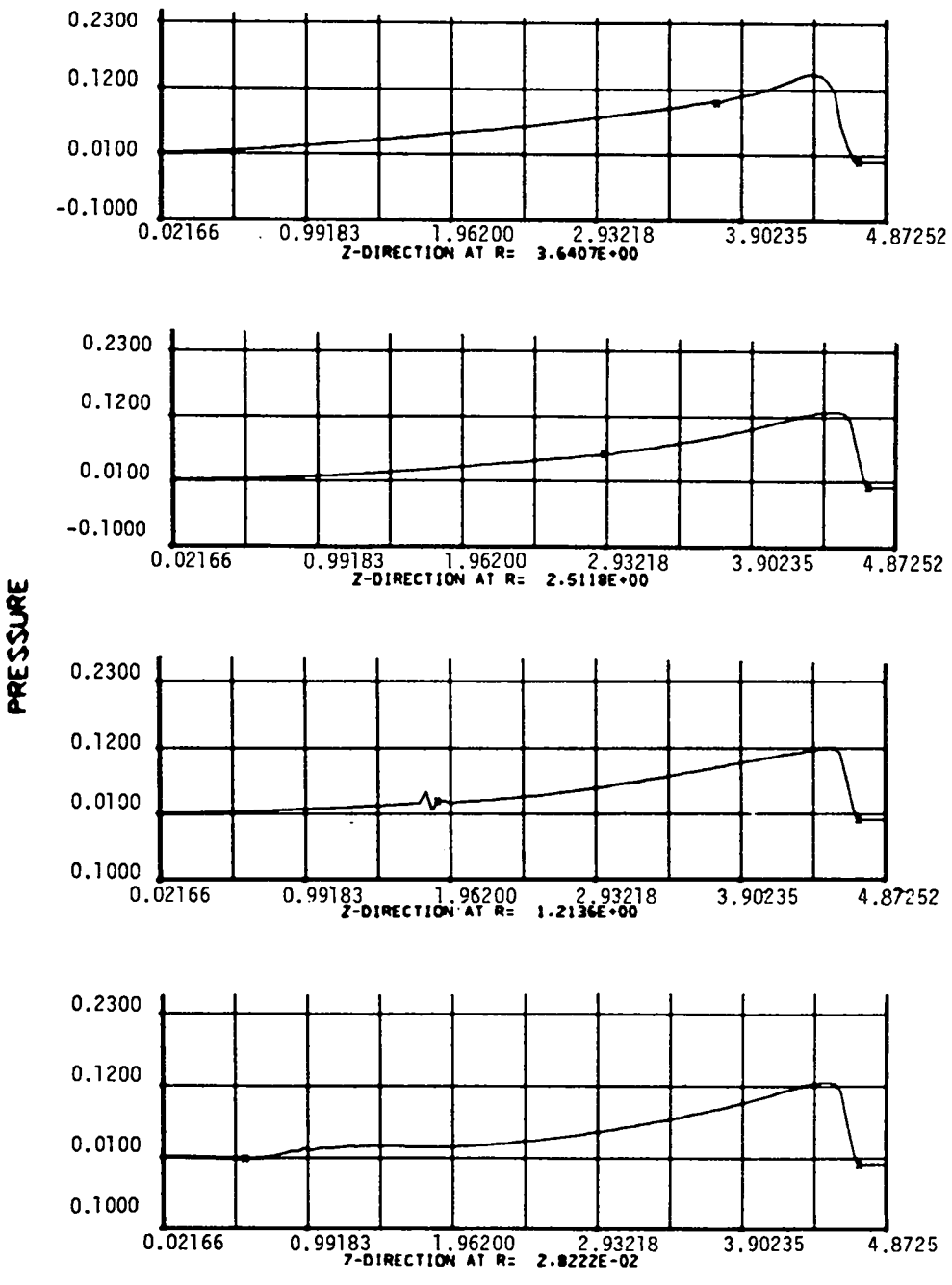

Fig. 7. Vertical one-dimensional pressure plots at given radii, t = 7.665 μs (P-040).

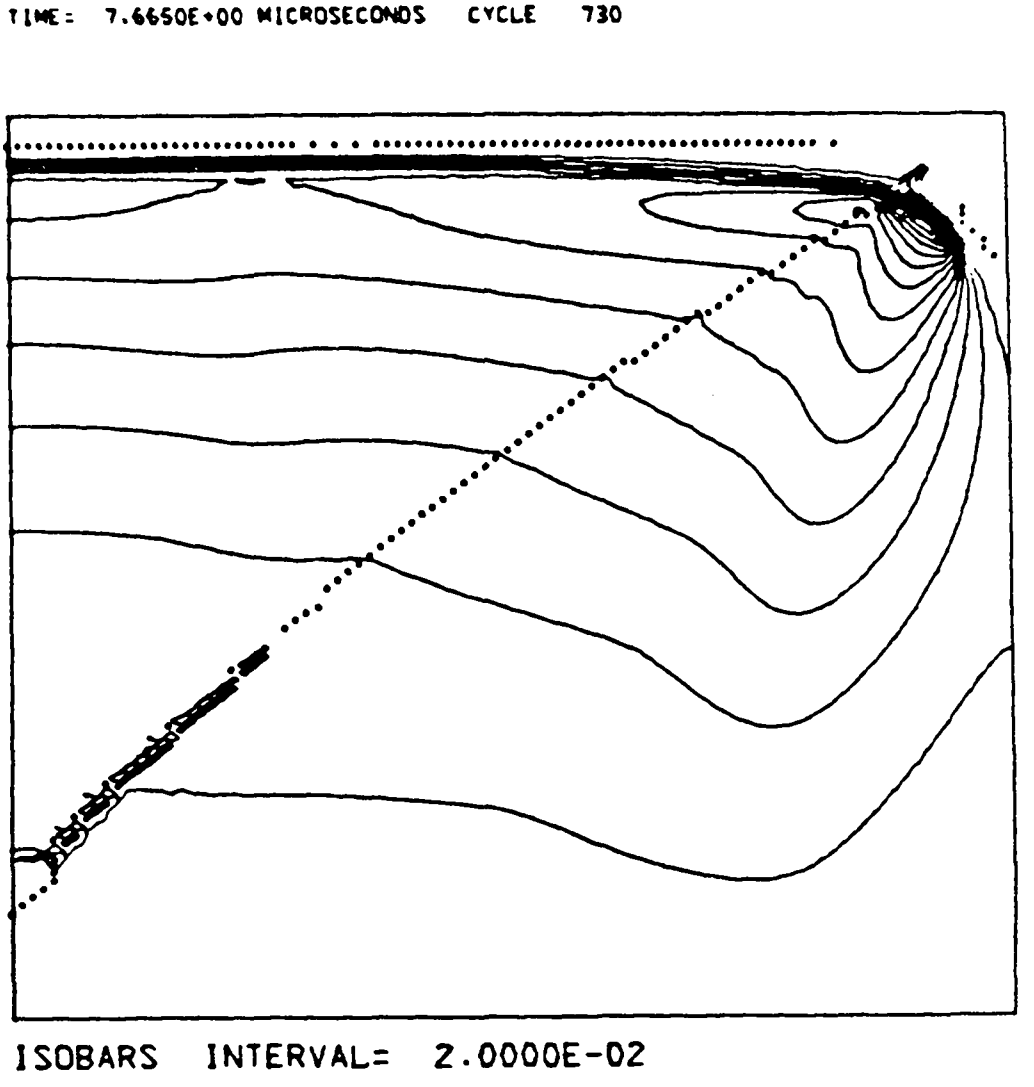

Fig. 8. Pressure contour plots at 7.665 μs (P-040).

Fig. 14 has a significant gradient across the lens, but the simultaneity of arrival, as shown in Figs. 14 and 15, is good. With the P-120, we have computed the most planar arriving wave in all of our plane wave generator calculations.

3. **Conclusions for the P-120 Plane Wave Generator.** The *calculated* aluminum plate, free-surface velocity varied from 1.8 mm/μs at 100-mm radius from the center to 1.77 mm/μs at the center of the plate. Experimental values of these same velocities were 1.75 and 1.62 mm/μs, respectively.[4] The calculated P-120 arriving shock wave is apparently flatter and has lower pressure gradients behind the detonation front and across the lens than is observed experimentally.

The calculated pressure gradients behind the detonation front depend critically upon the angle used for the diagonal between the Baratol and the Comp B. The lower plate velocity at the center of the lens, for the design with 40° for the diagonal, becomes the highest plate velocity for a design in which this angle is changed to 37.5°, according to our calculations. The P-120 lens studied by Ramsay[4] has several changes or undulations in the Comp B/Baratol diagonal interface (varying from 37.5° to 40°) to compensate for variability in performance of the explosive charges resulting from manufacturing inaccuracies.

Thus the calculated pressure gradient across the P-120 lens depends upon an uncertain geometry and composition.

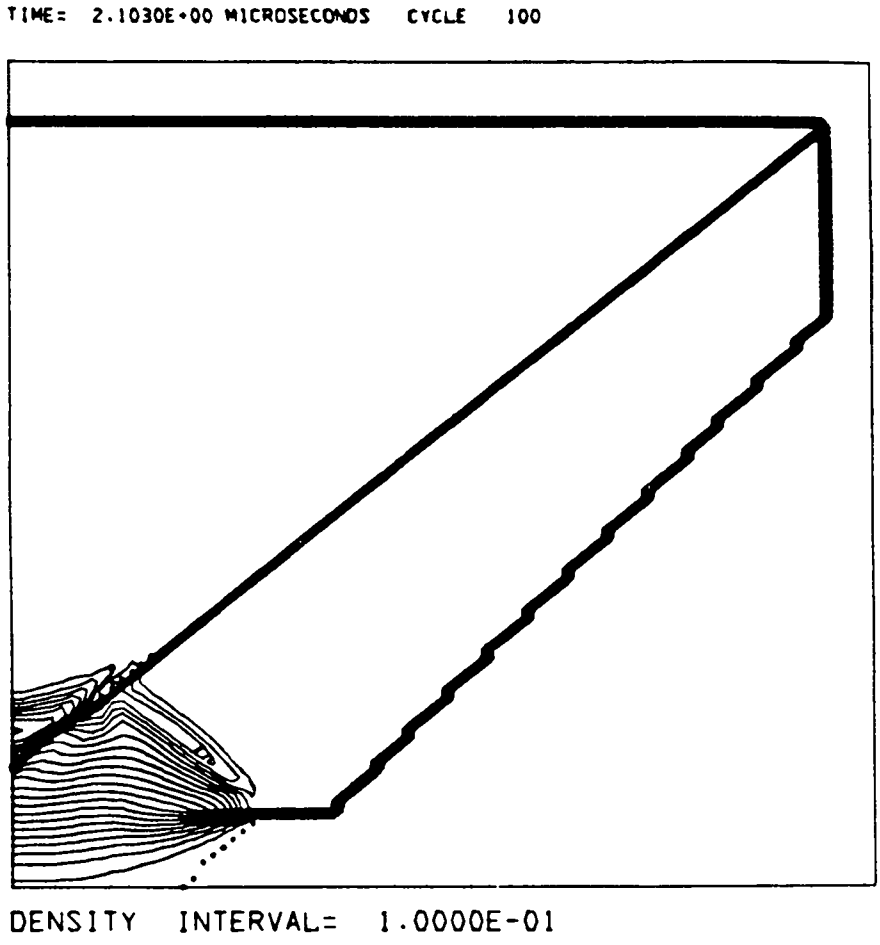

Fig. 9a. Density contour plots at 2.103 μs (P-081).

V. GENERAL CONCLUSIONS

We conclude that, although the detonation wave arrives almost planar across the top of the lens, a significant gradient is present across the lens and behind the wave surface. We also conclude that the pressure gradients depend significantly upon the geometry and composition variables, which are difficult to control during manufacture. Thus the calculated pressure gradients across the lens are probably less steep than those actually present in most plane wave generators.

Experimental data[4] suggest that the pressure profile behind the front is asymmetrically oriented with respect to the charge center, which may adversely affect wedge shock initiation (Pop plot) experiments.

Magnitude variations, calculated and observed, prevent obtaining high-quality shock-initiation data, particularly for the more shock-insensitive explosives. Plane wave generator improvement will require quality control tests for *both* the arrival trace (planarity) and the pressure distribution. It may be necessary to await advances in the design of plane wave generators.

ACKNOWLEDGMENTS

The authors recognize and value the contributions of John B. Ramsay, Harry L. Flaugh, Agapito P. Torres, George G. Hill, Raymond D. Steele, and James D. Kershner.

REFERENCES

1. James D. Kershner and Charles L. Mader, "2DE, a Two-Dimensional Continuous Eulerian

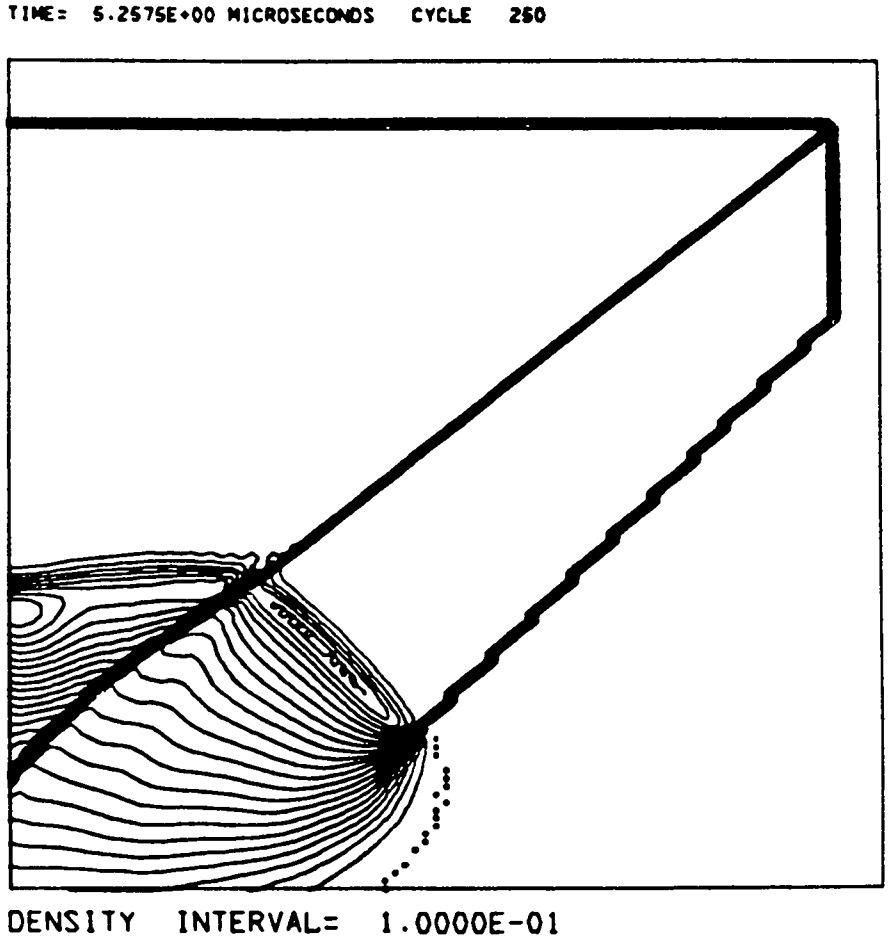

Fig. 9b. Density contour plots at 5.2575 μs (P-081).

Hydrodynamic Code for Computing Multicomponent Reactive Hydrodynamic Problems," Los Alamos Scientific Laboratory report LA-4846 (March 1972).

2. George H. Pimbley and Elisabeth F. Marshall, "The Premature Detonation Problem," Los Alamos Scientific Laboratory report LA-8352-MS (May 1980).
3. Charles L. Mader, *LASL PHERMEX Data, Vol. II* (University of California Press, Berkeley, 1980).
4. John B. Ramsay, "Nonplanar Pressure Distribution in P-120 Systems," Los Alamos Scientific Laboratory, Group M-3, memorandum to H. L. Flaugh, September 29, 1980.

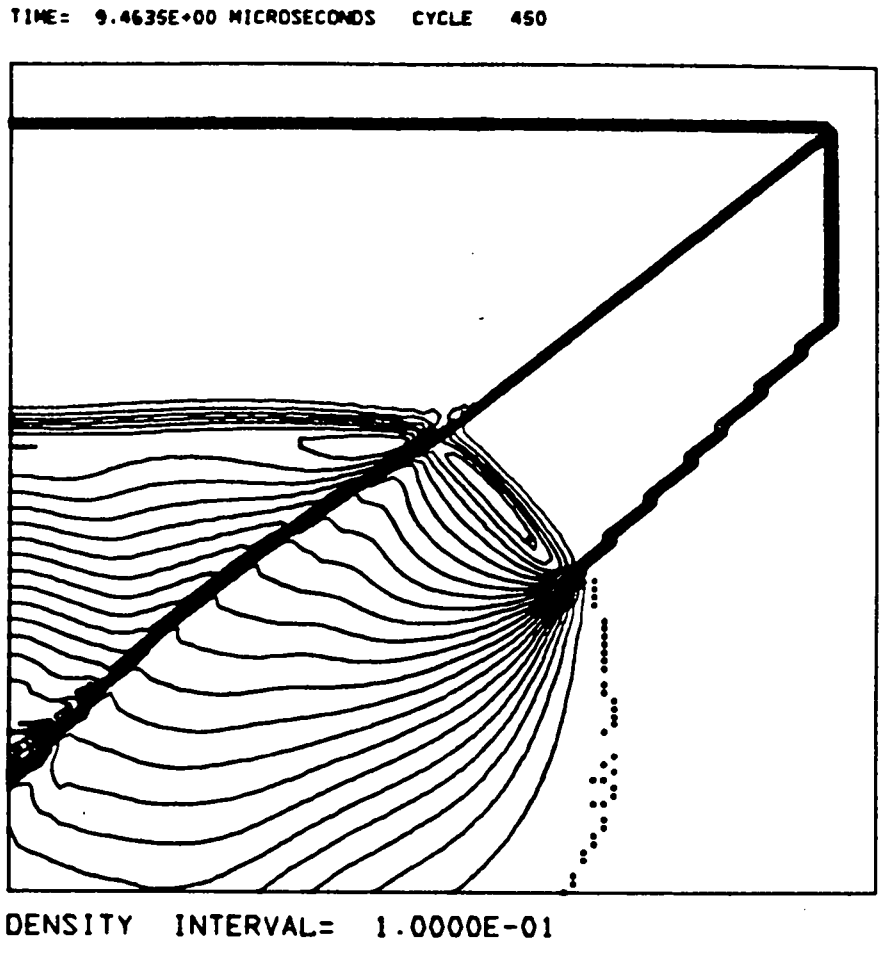

Fig. 9c. Density contour plots at 9.4635 μs (P-081).

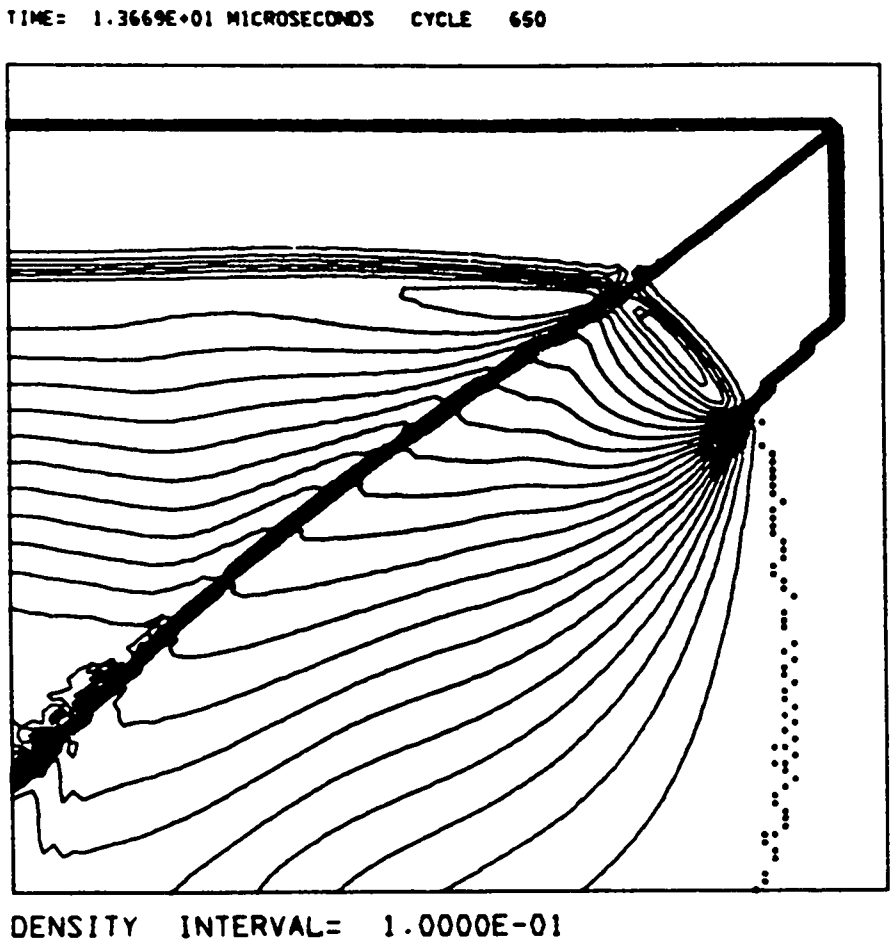

Fig. 9d. Density contour plots at 13.669 μs (P-081).

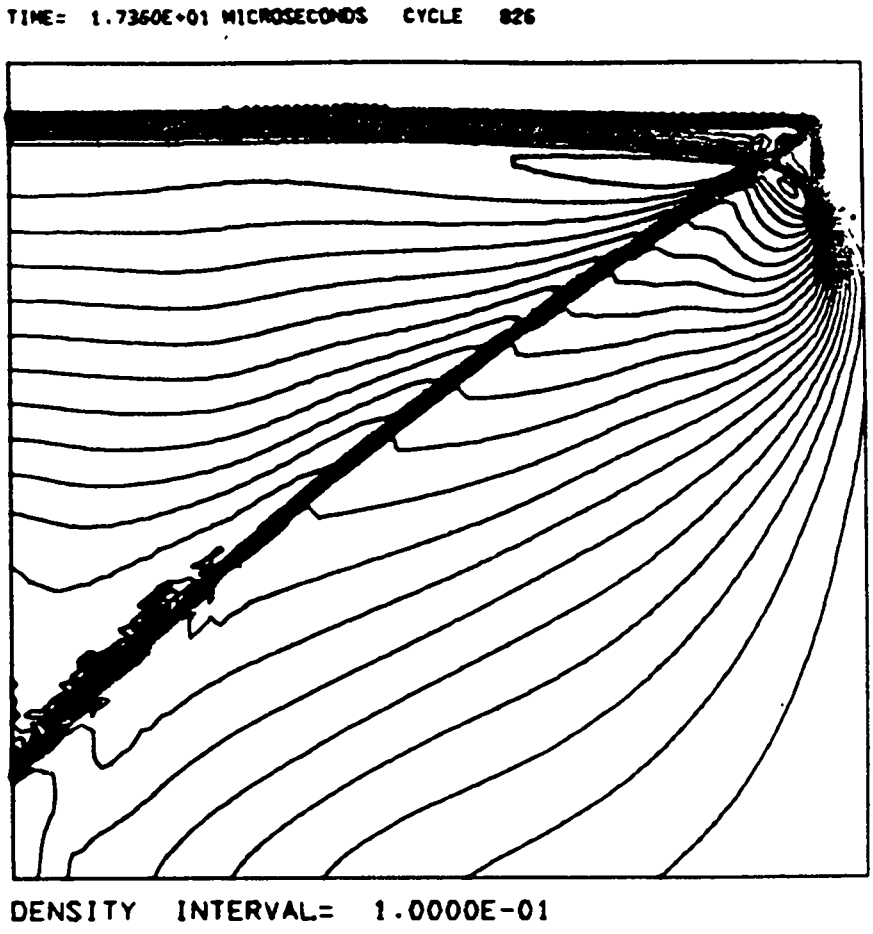

Fig. 9e. Density contour plots at 17.35 μs (P-081).

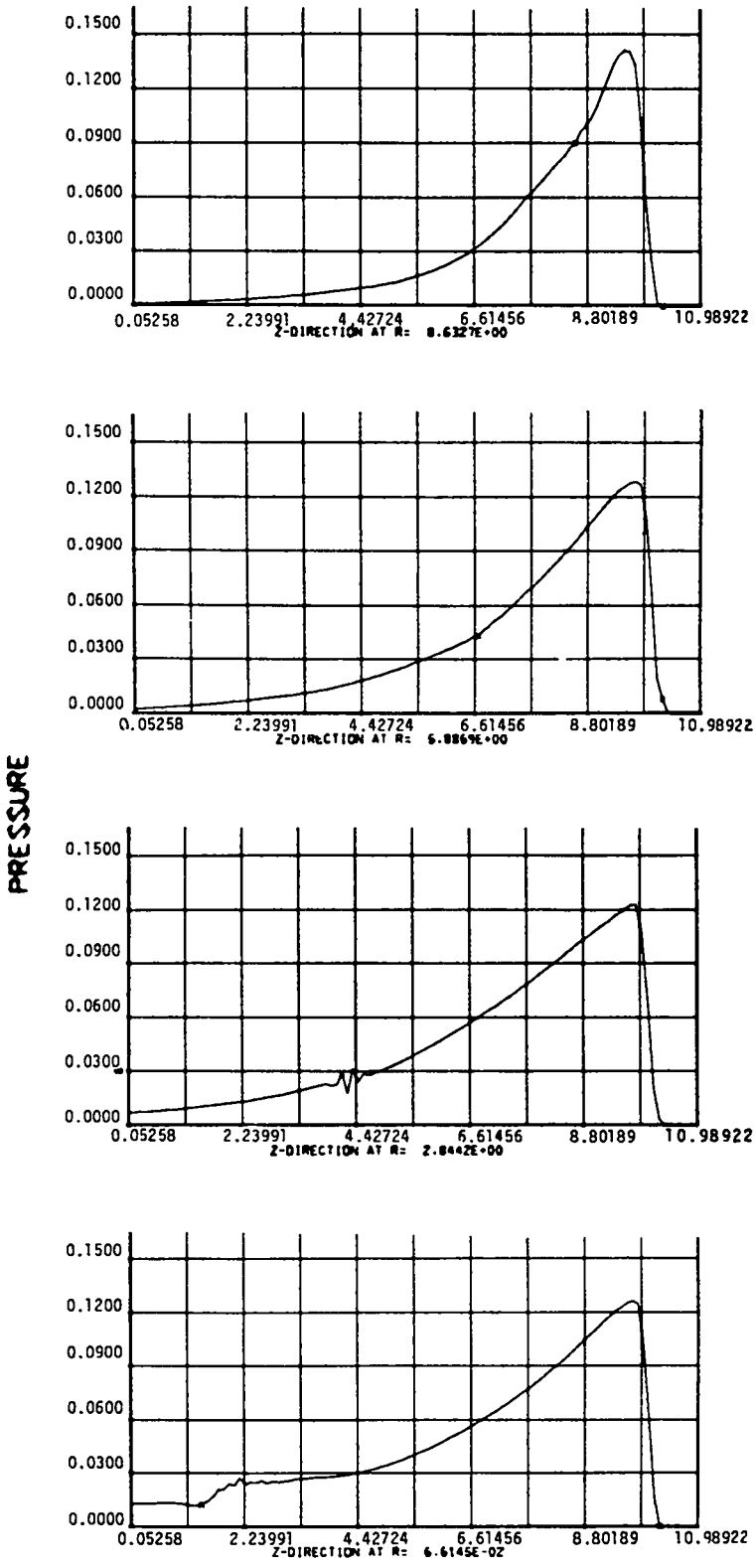

Fig. 10. Vertical one-dimensional pressure plots at given radii, t = 17.35 μs (P-081).

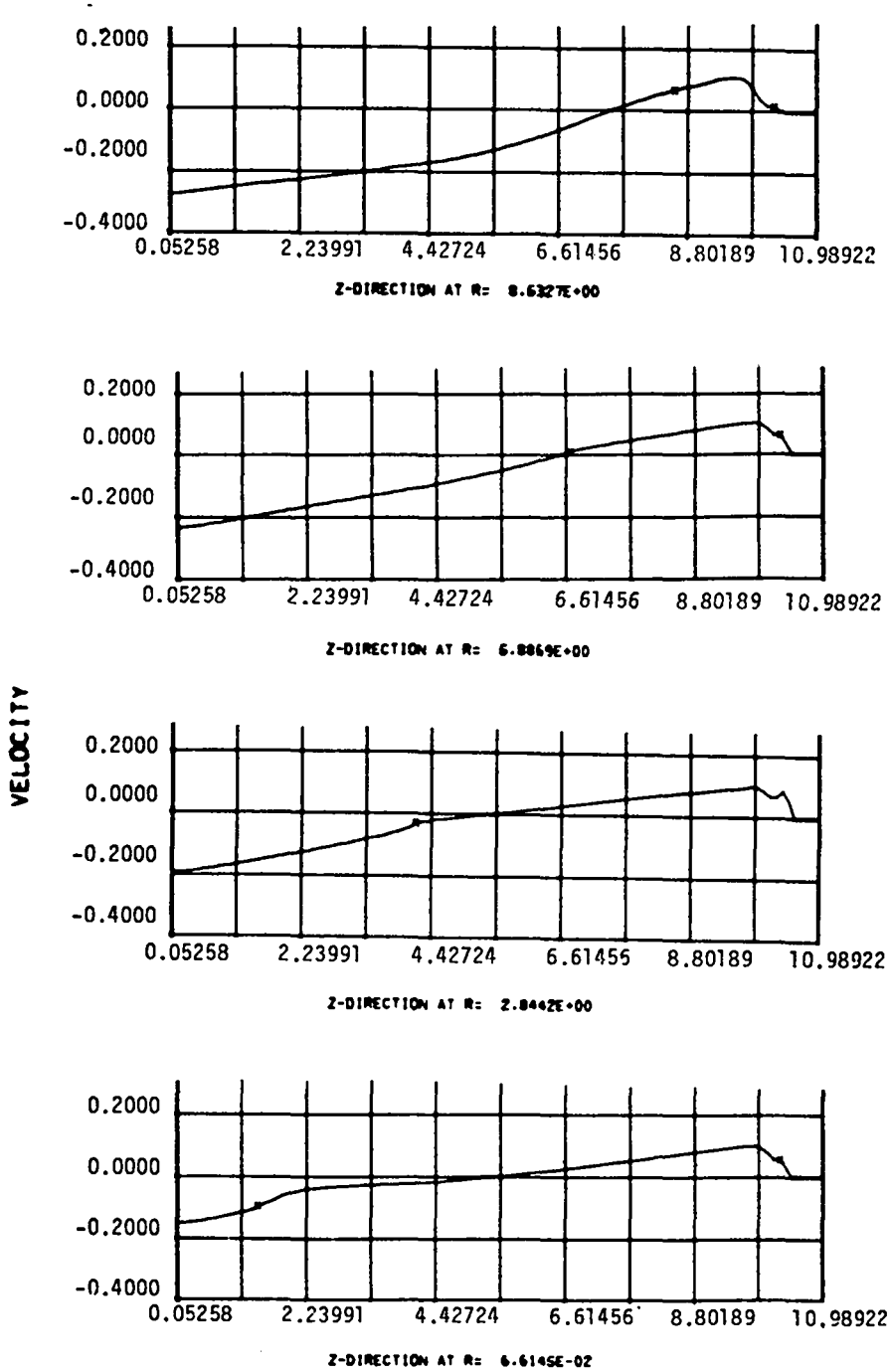

Fig. 11. Vertical one-dimensional velocity plots at given radii, t = 17.35 μs (P-081).

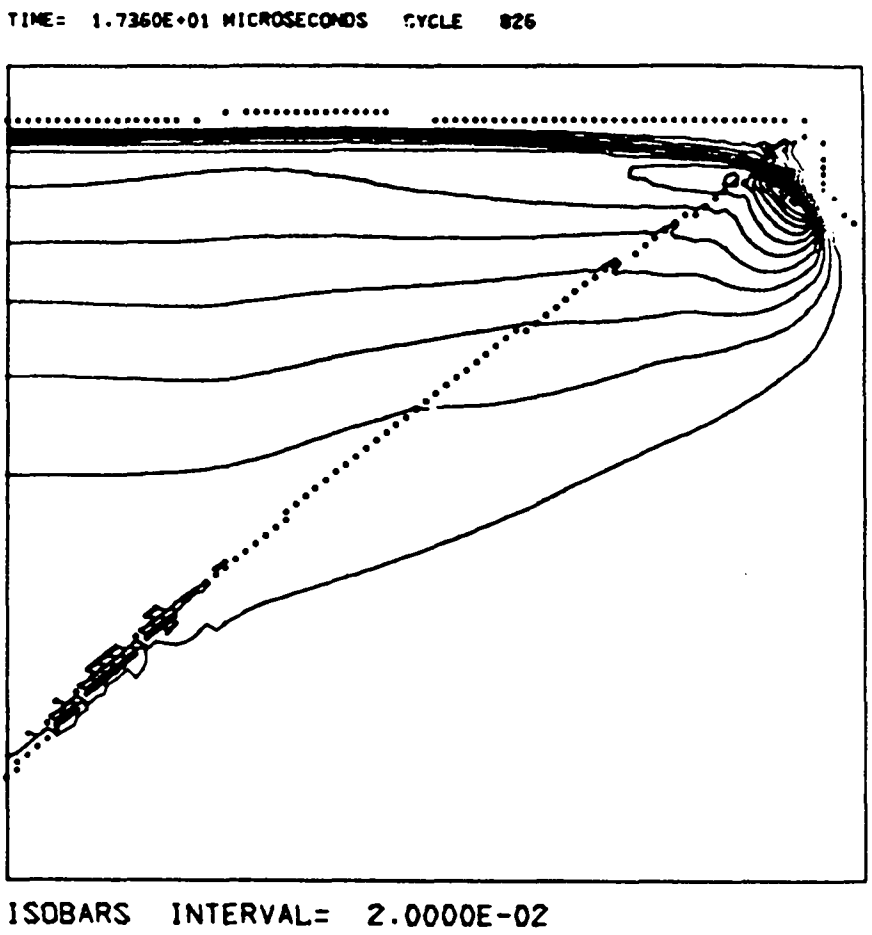

Fig. 12. Pressure contour plots at 17.35 μs (P-081).

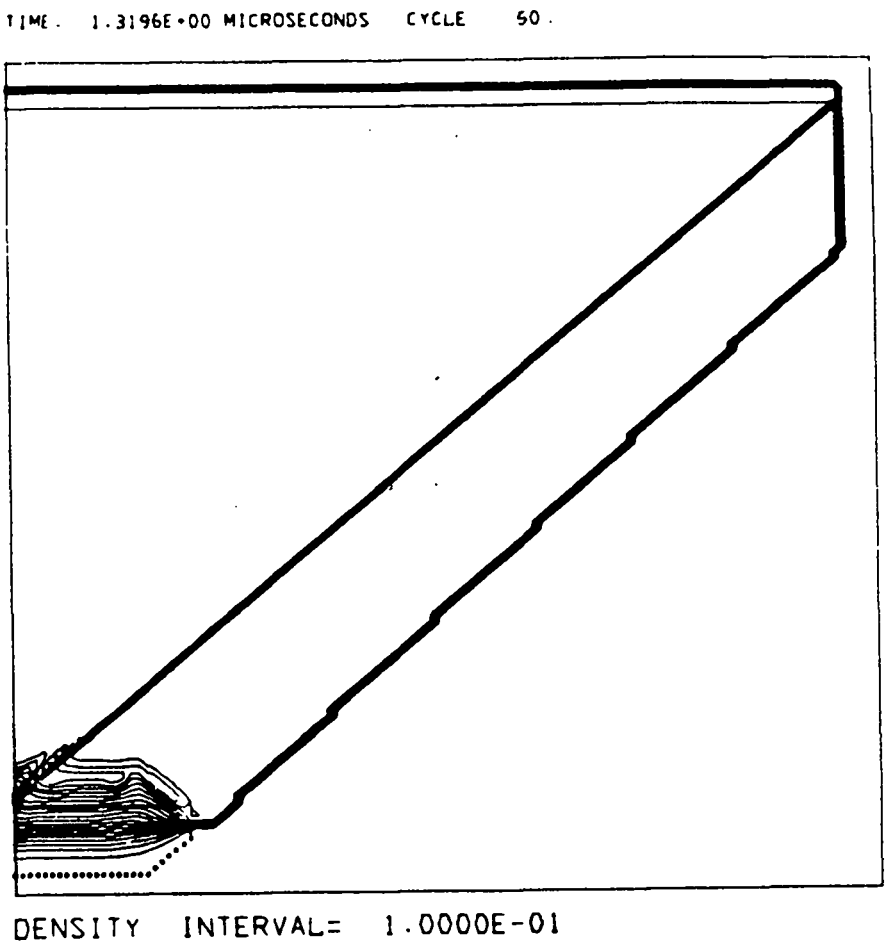

Fig. 13a. Density contour plots at 1.3196 μs (P-120).

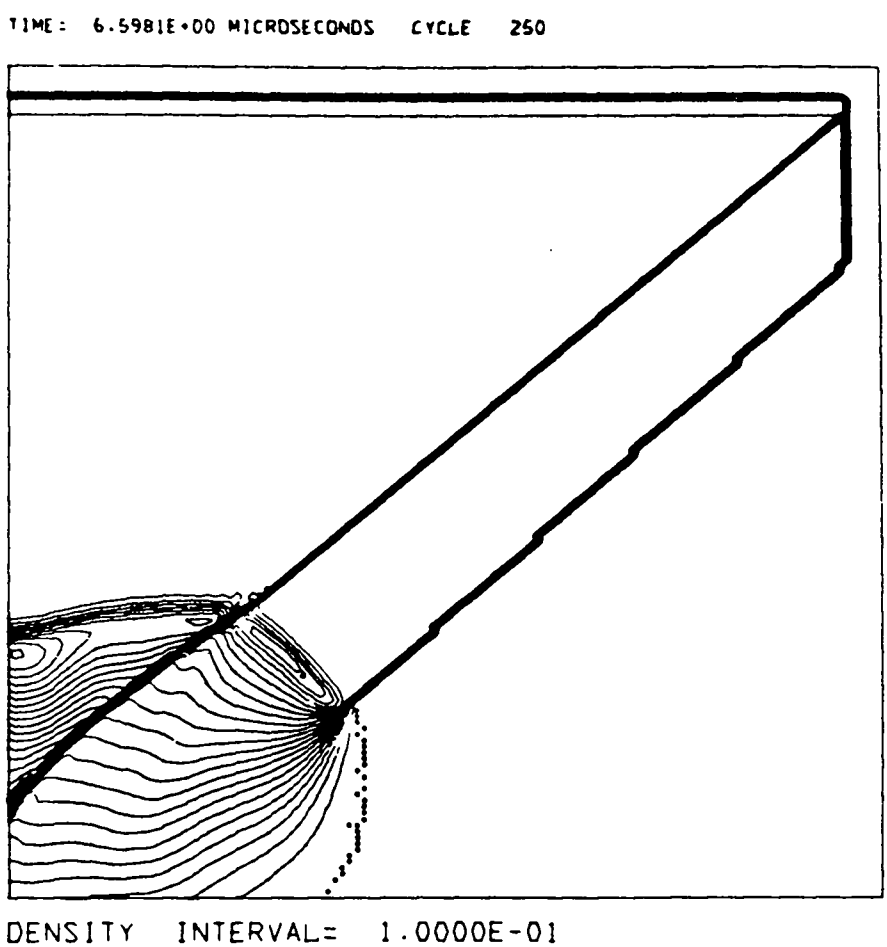

Fig. 13b. Density contour plots at 6.5981 μs (P-120).

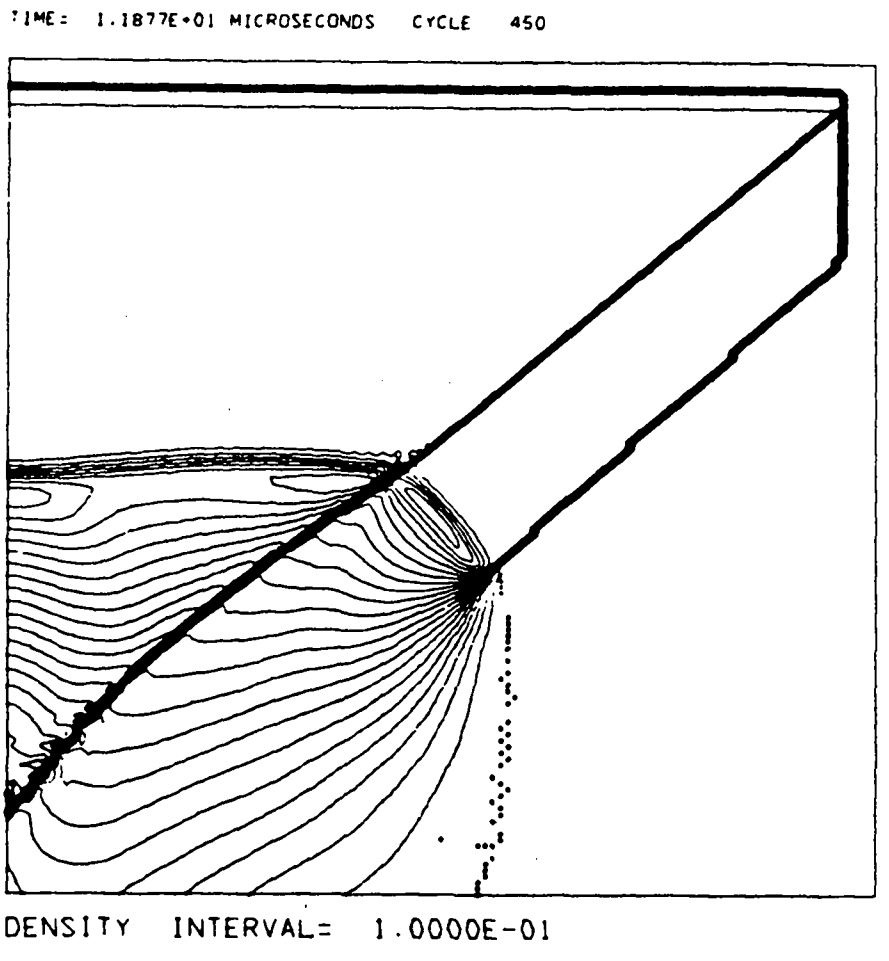

Fig. 13c. Density contour plots at 11.877 μs (P-120).

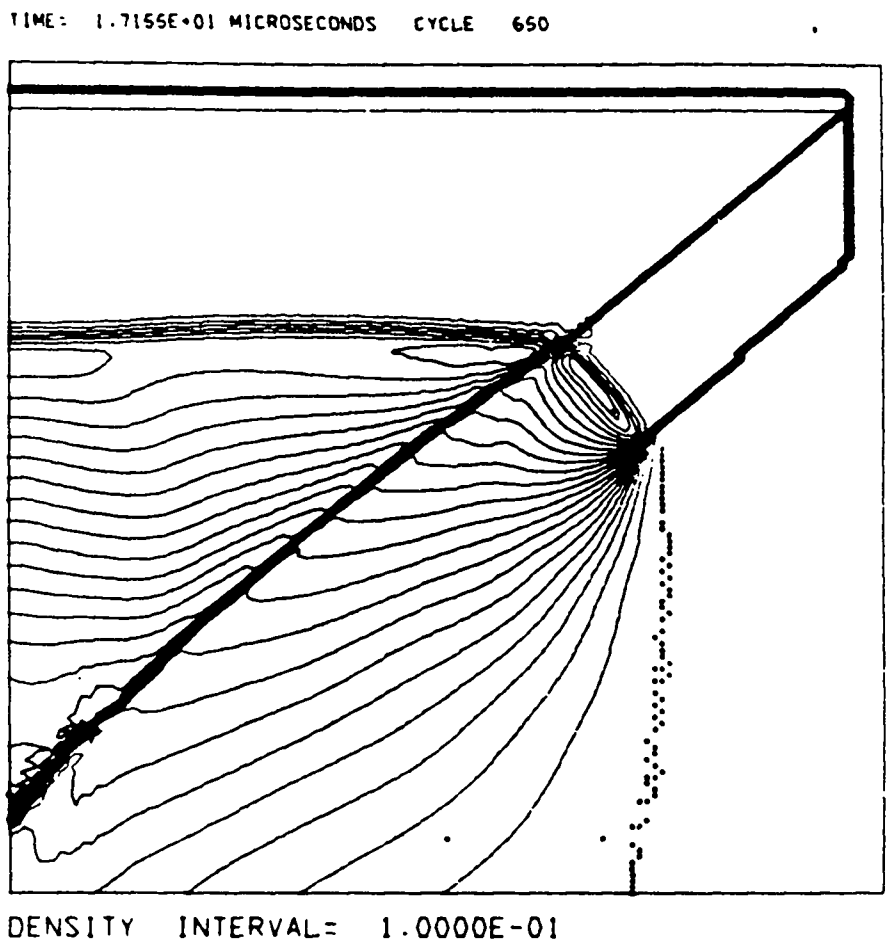

Fig. 13d. Density contour plots at 17.155 μs (P-120).

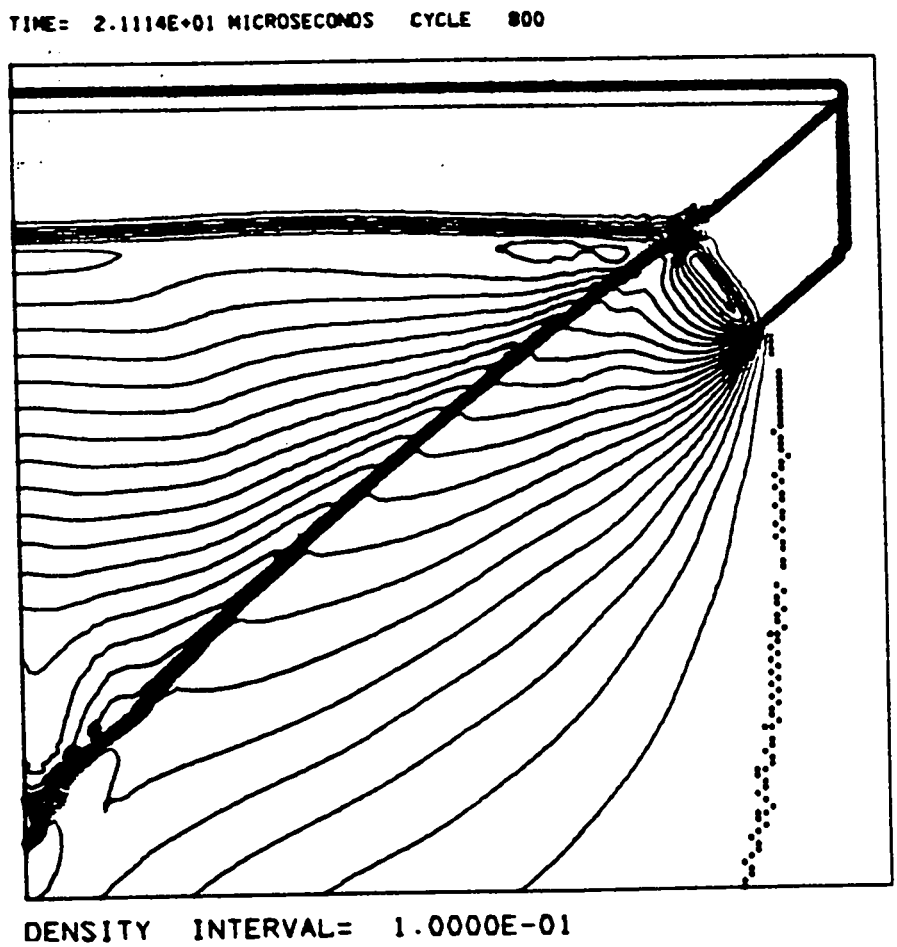

Fig. 13e. Density contour plots at 21.114 μs (P-120).

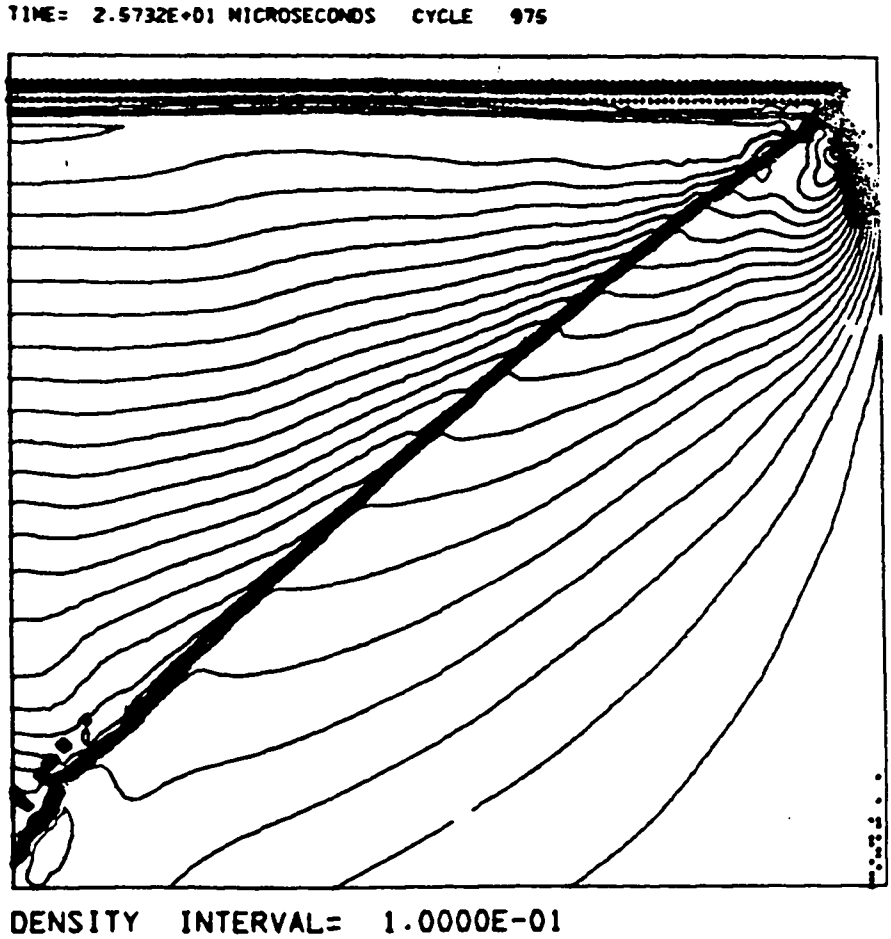

Fig. 13f. Density contour plots at 25.732 μs (P-120).

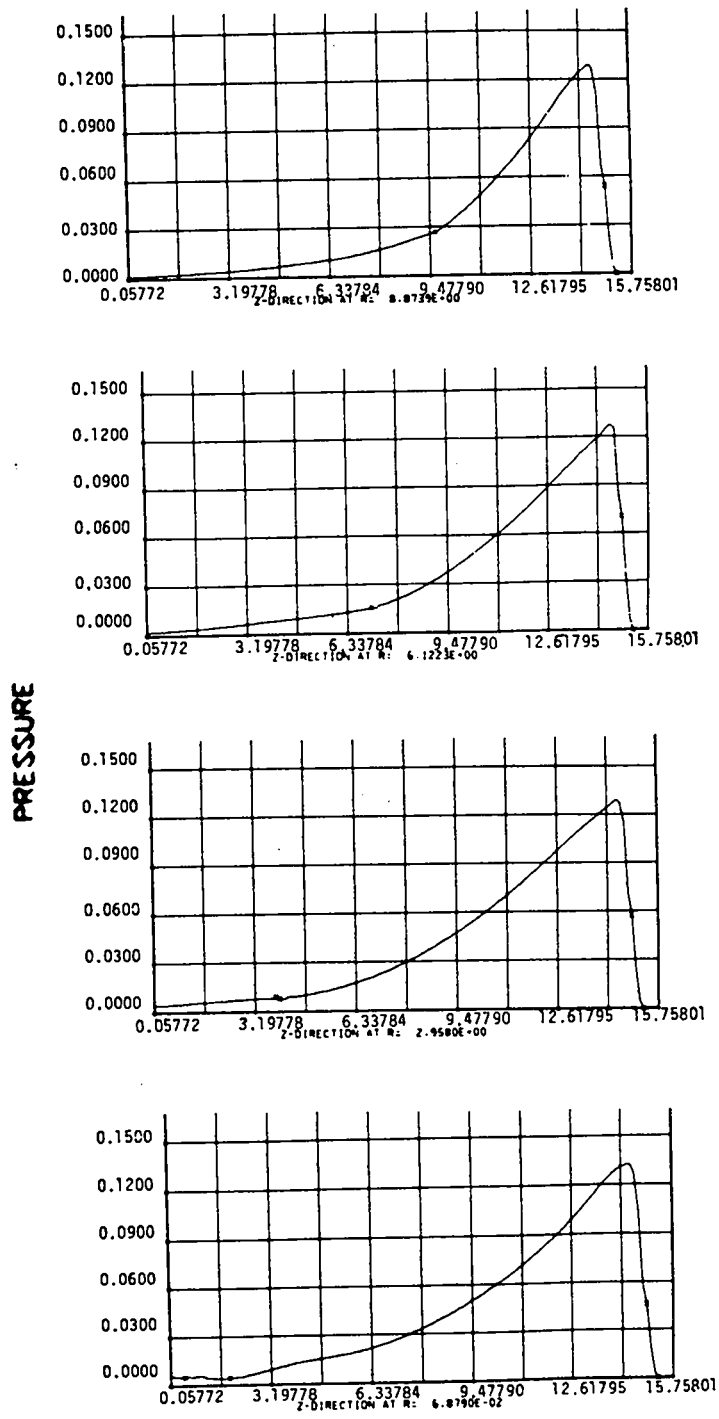

Fig. 14. Vertical one-dimensional pressure plots at given radii, t = 25.732 μs (P-120).

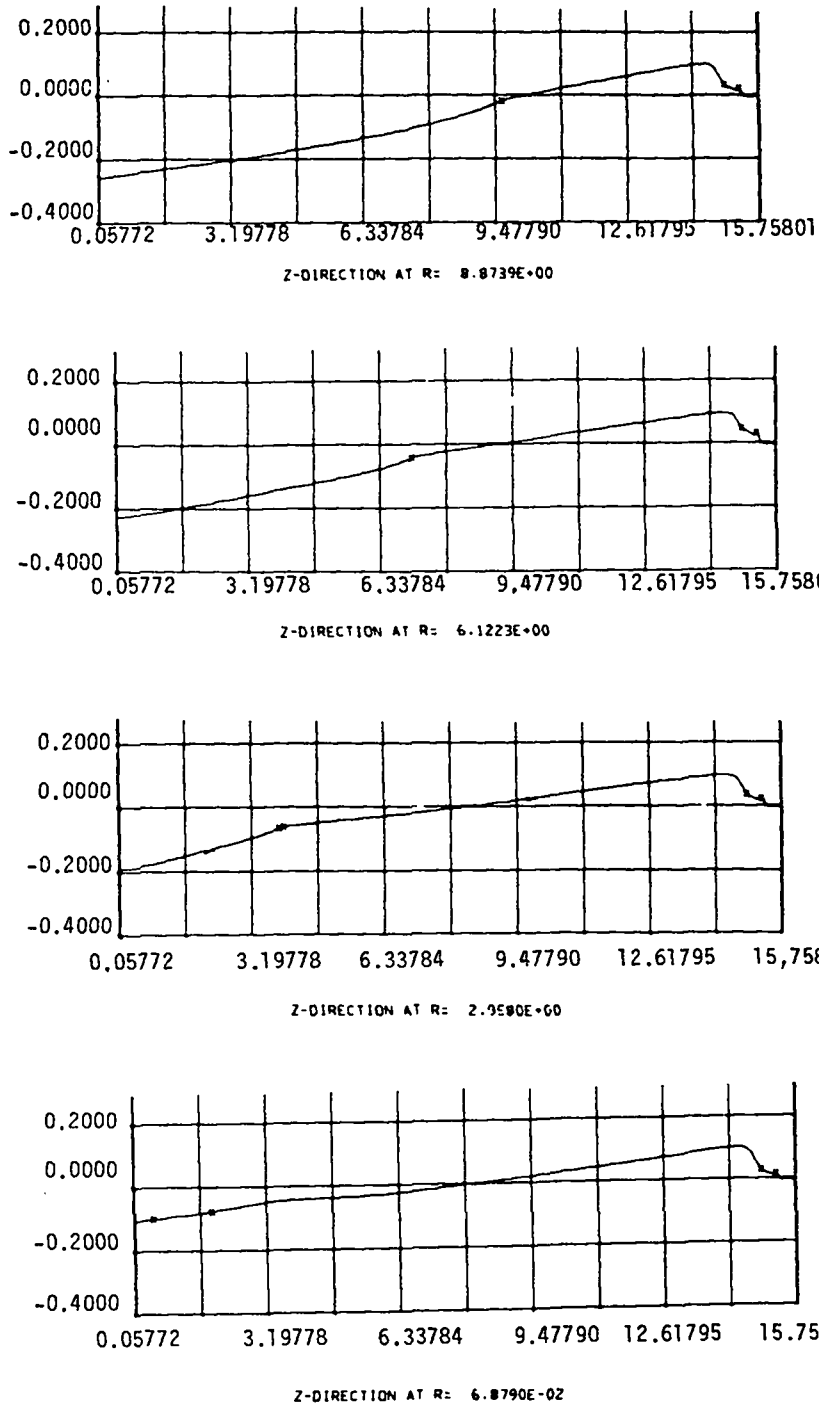

Fig. 15. Vertical one-dimensional velocity plots at given radii, t = 25.732 μs (P-120).

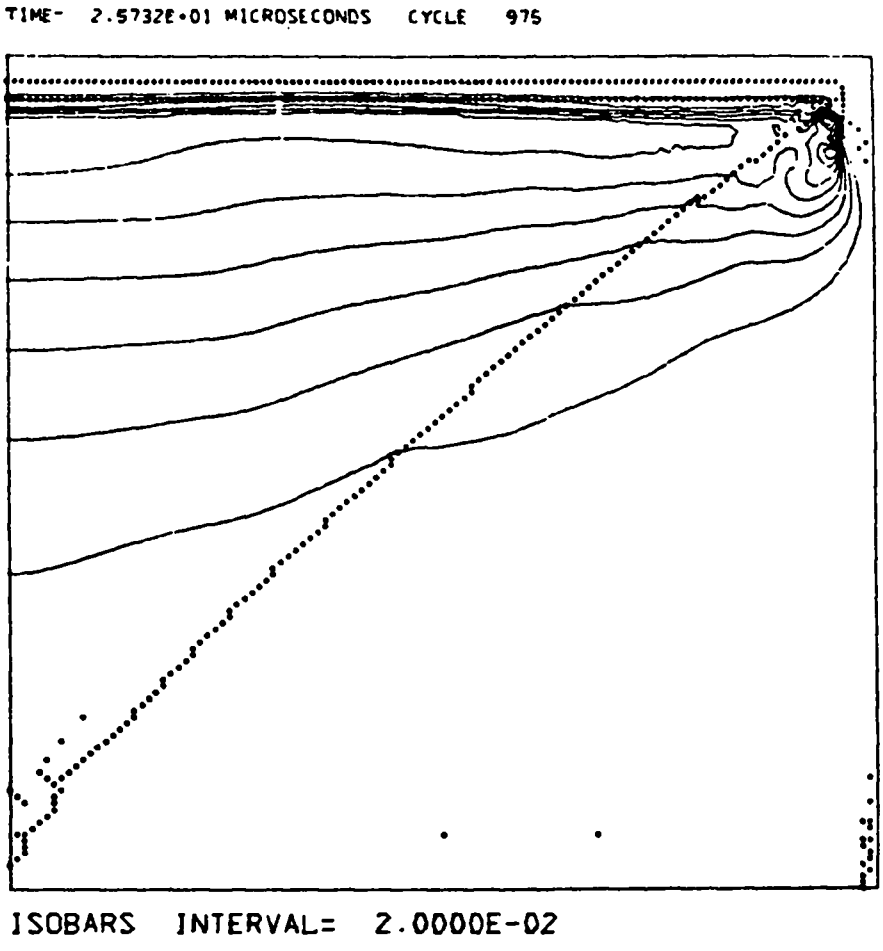

Fig. 16. Pressure contour plots at 25.732 μs (P-120).

Printed in the United States of America
Available from
National Technical Information Service
US Department of Commerce
5285 Port Royal Road
Springfield, VA 22161

Microfiche $3.50 (A01)

Page Range	Domestic Price	NTIS Price Code	Page Range	Domestic Price	NTIS Price Code	Page Range	Domestic Price	NTIS Price Code	Page Range	Domestic Price	NTIS Price Code
001-025	$ 5.00	A02	151-175	$11.00	A08	301-325	$17.00	A14	451-475	$23.00	A20
026-050	6.00	A03	176-200	12.00	A09	326-350	18.00	A15	476-500	24.00	A21
051-075	7.00	A04	201-225	13.00	A10	351-375	19.00	A16	501-525	25.00	A22
076-100	8.00	A05	226-250	14.00	A11	376-400	20.00	A17	526-550	26.00	A23
101-125	9.00	A06	251-275	15.00	A12	401-425	21.00	A18	551-575	27.00	A24
126-150	10.00	A07	276-300	16.00	A13	426-450	22.00	A19	576-600	28.00	A25
									601-up	†	A99

†Add $1.00 for each additional 25-page increment or portion thereof from 601 pages up.

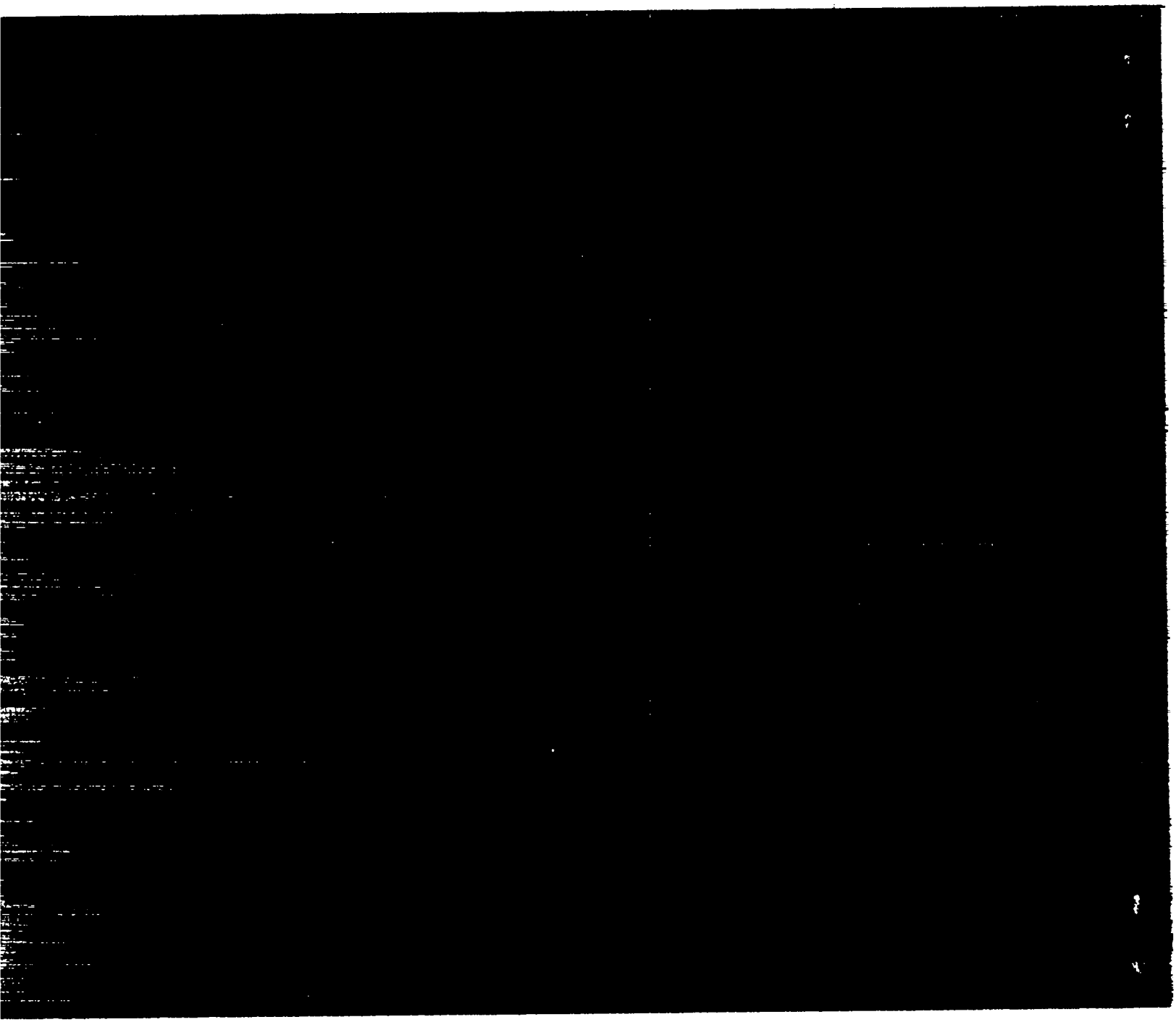

Los Alamos